Cell Reports, Volume *33*

Supplemental Information

Rapid Precision Functional Mapping of Individuals Using Multi-Echo fMRI

Charles J. Lynch, Jonathan D. Power, Matthew A. Scult, Marc Dubin, Faith M. Gunning, and Conor Liston

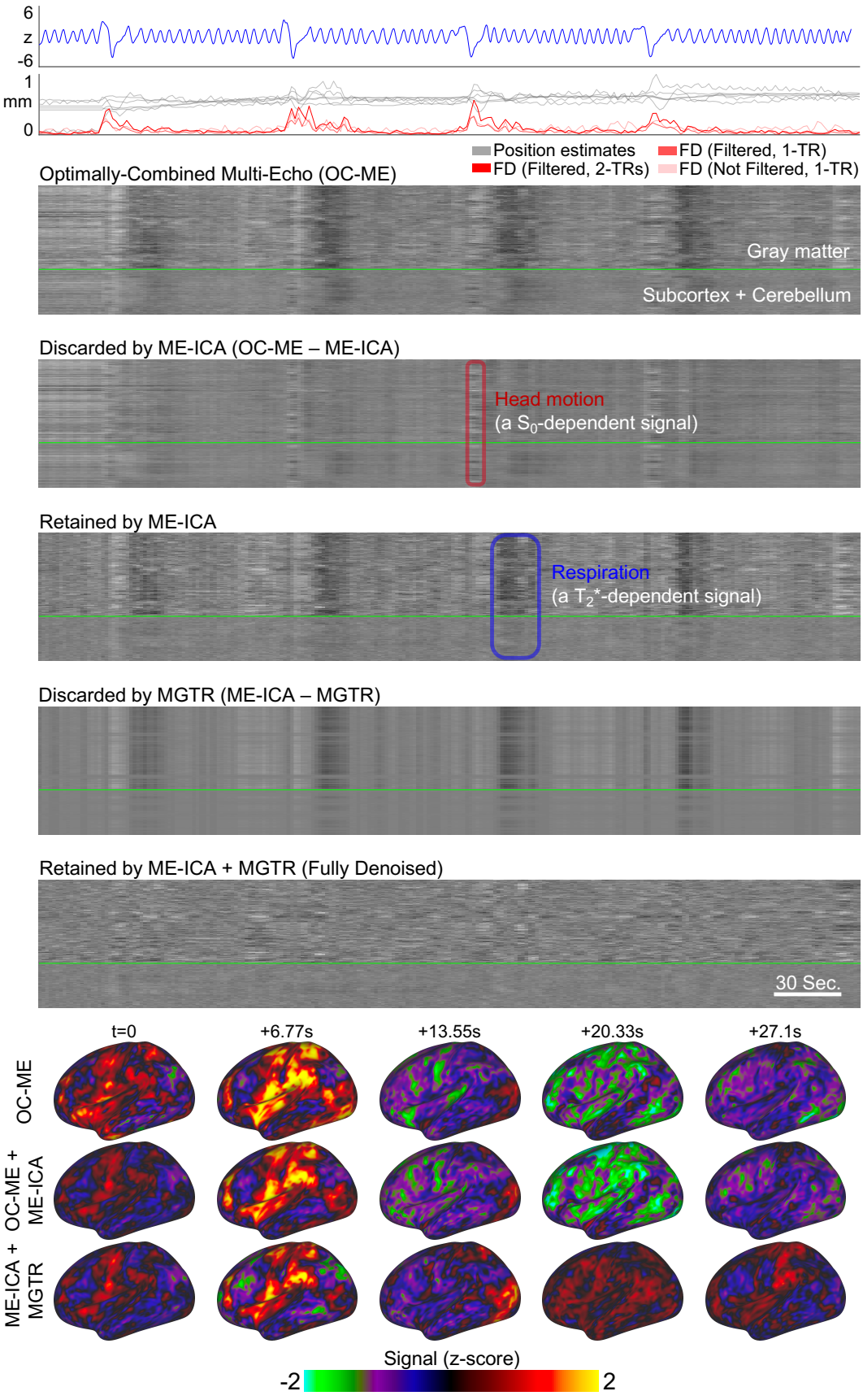
6
z
-6
1
mm
0
Position estimates
FD (Filtered, 2-TRs)
FD (Filtered, 1-TR)
FD (Not Filtered, 1-TR)
Optimally-Combined Multi-Echo (OC-ME)
Gray matter
Subcortex + Cerebellum
Discarded by ME-ICA (OC-ME – ME-ICA)
Head motion
(a S0-dependent signal)
Retained by ME-ICA
Respiration
(a T2*-dependent signal)
Discarded by MGTR (ME-ICA – MGTR)
Retained by ME-ICA + MGTR (Fully Denoised)
30 Sec.
t=0
+6.77s
+13.55s
+20.33s
+27.1s
OC-ME
OC-ME + ME-ICA
ME-ICA + MGTR
Signal (z-score)
-2
2

Figure S1. Related to Figure 3. An event-related approach for establishing appropriate separation of neurobiological (T_2*-dependent; "BOLD-like") and non-neurobiological (S_0-dependent; not "BOLD-like") fMRI signals. During each instructed deep breathing scan, sub-ME01 was prompted every 70 seconds (via a visual cue) to take a deep breath. There are prominent T_2*- and S_0-dependent signals with predictable spatiotemporal characteristics (each described in turn below) associated with deep breaths that are visually evident when these scans are viewed as "gray plots" (Power, 2017) paired with head motion and respiration belt traces. Respiration (measured using an abdominal belt sampling at 50 Hz; z = z-score) and head motion (frame-wise displacement; filtered realignment parameters and calculated over two TRs instead of one; as done in (Power, 2019)) are shown at the top of Fig. S1 as a blue and red traces, respectively. The time-courses of all points in the brain before and after each denoising step are shown below these traces as gray plots (Power, 2017), with white and black representing high and low signal values, respectively. Four isolated deep breaths, each accompanied by a transient spike in head motion and followed by pauses in ventilation, are visually apparent in an otherwise eupneic trace. For each of these respiratory events, there is an increase in head motion, which manifests visually in the gray plot as a vertical "salt-and-pepper" band time-locked to the deep breath. Because head movement primarily influences S_0 and not T_2*, these signals are discarded by ME-ICA (second gray plot; red box), as expected. Deep breaths also alter the concentration of carbon dioxide in blood, however, which in turn influences cerebral blood flow (Hall and Guyton, 2011), and therefore T_2* and not S_0. Vertical black bands (represented most strongly in gray matter) lasting tens of seconds after each deep breath, consistent with the expected cortex-wide decrease in blood flow after a transient increase in ventilation, are retained by ME-ICA (third gray plot; blue box). While this observation indicates the desired retention of T_2*-dependent signals, it also highlights a limitation that is inherent to ME-ICA. Specifically, that although cortex-wide fluctuations in signal due to changes in respiration are not a signal of interest per se, they are retained in the ME-ICA denoised time-series nonetheless because they are T_2*-dependent (in addition, ICA techniques cannot easily separate spatially diffuse signals from focal signals; see (Power et al., 2019; Power et al., 2018)). Thus, additional denoising procedures (e.g., mean grey matter time-series regression; MGTR) are required to remove them. ME-ICA paired with MGTR yields an fMRI time-series free of the confounding influence of head motion (as well as other S_0-dependent artifacts) and respiration (fifth gray plot). These gray plots indicate appropriate separation of S_0- and T_2*-dependent signals of interest using ME-ICA and MGTR. To better understand the spatiotemporal profile of the signals that were discarded and retained by ME-ICA, we extracted the average 40 second (-10 seconds to 30 seconds) epoch surrounding deep

breaths. These data are displayed on the subject's inflated cortical surface at the bottom of Fig. S1. The motion-related artifact at t=0 (this is the S_0-dependent "salt-and-pepper" band bounded by the red box in the OC-ME – ME-ICA gray plot; red box) is present in the OC-ME time-series but not the ME-ICA denoised time-series. The spatially diffuse decrease in signal begins approximately 14 seconds after the deep breath cue (this is the T_2*-dependent vertical black band bounded by the blue box in the ME-ICA gray plot), and is retained in the ME-ICA time-series and only removed by MGTR.

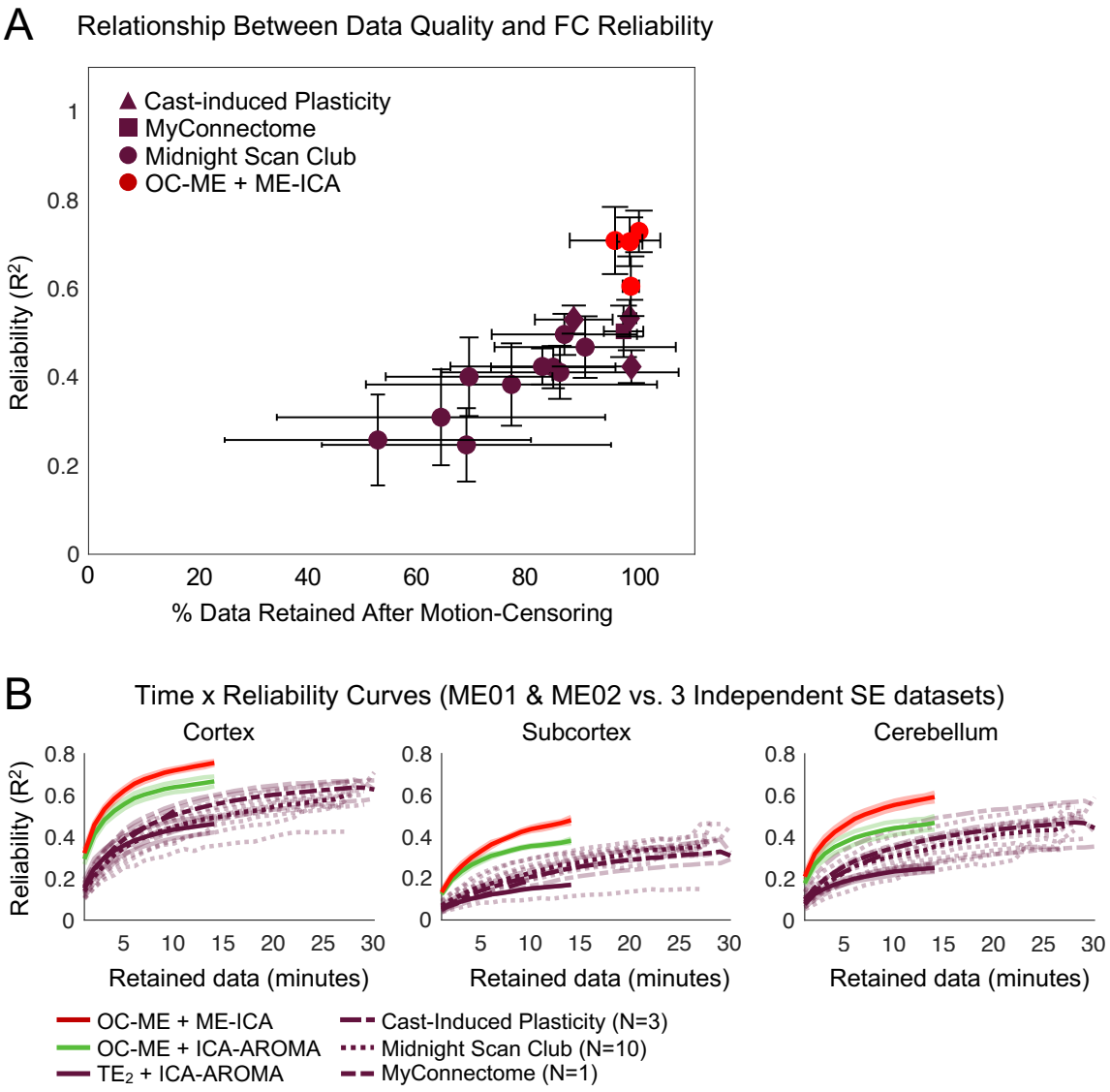

Figure S2. Related to Figure 3. FC reliability values calculated using data from the first ten minutes of scanning (the minimum scan duration across all four datasets) plotted relative to the percentage of data retained after motion-censoring in Fig. S2A. Error bars indicate standard deviation. A subset of MSC participants (purple circles) exhibiting high levels of head movement (and less data retained after motion-censoring) exhibited the worst FC reliability. OC-ME + ME-ICA data (the red circles in Fig. S2A) yielded better FC reliability values than MyConnectome and CAST single-echo data with an equivalent level of motion-censoring. An alternative set of time x reliability curves (where the x-axis represents the amount data retained after motion-censoring and not the scan duration prior to motion-censoring) is presented in Fig. S2B . This analysis yielded a very similar set of curves as in Fig. 3B (with the exception of participants exhibiting

especially high levels of head motion; e.g., sub-MSC08). Collectively, these two analyses indicate that the enhanced reliability of FC measurements in the N=4 multi-echo dataset cannot be explained by head movement levels.

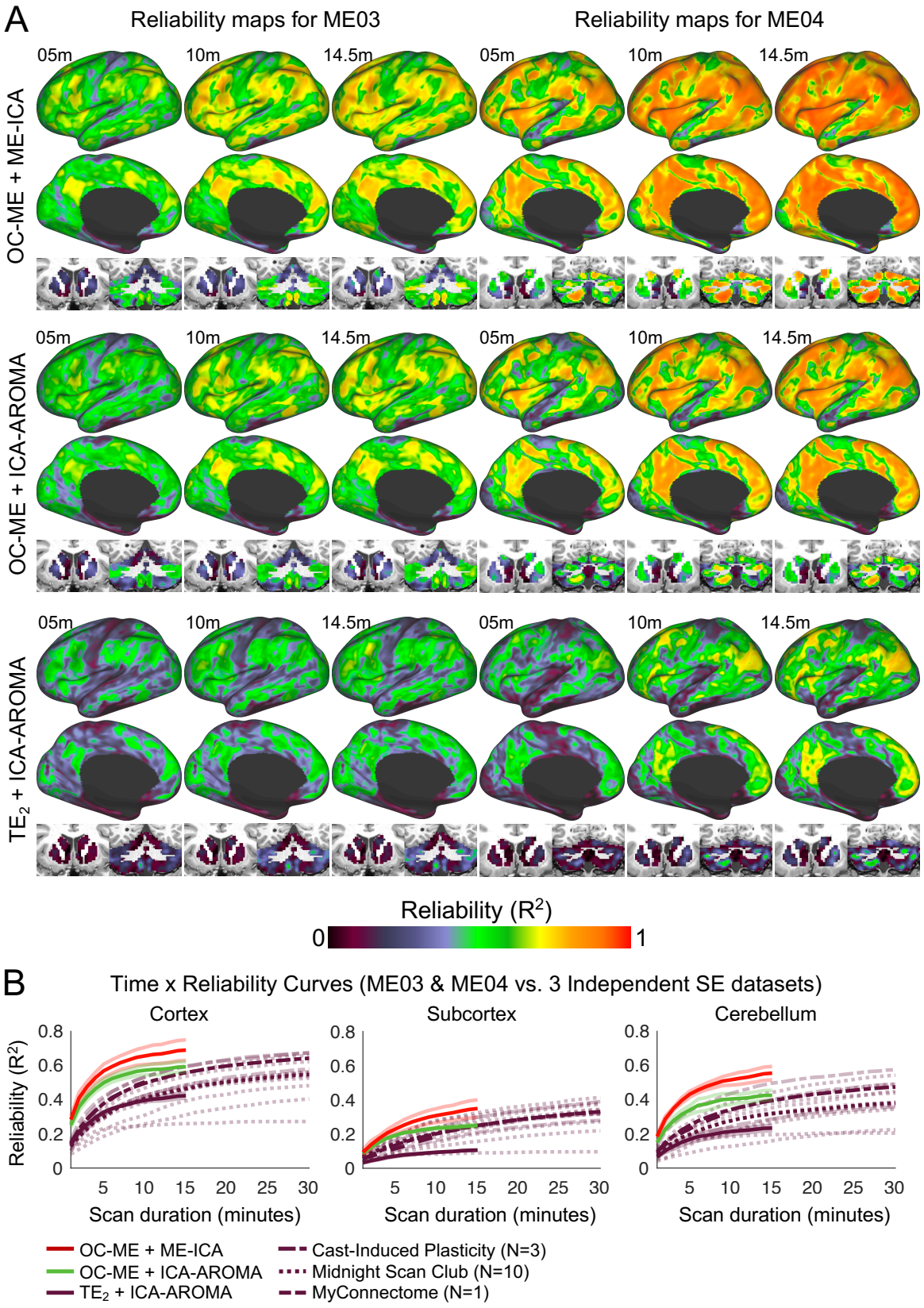
A
Reliability maps for ME03
Reliability maps for ME04
05m
10m
14.5m
OC-ME + ME-ICA
OC-ME + ICA-AROMA
TE2 + ICA-AROMA
Reliability (R2)
0
1
B
Time x Reliability Curves (ME03 & ME04 vs. 3 Independent SE datasets)
Cortex
Subcortex
Cerebellum
Reliability (R2)
0.8
0.6
0.4
0.2
0
5
10
15
20
25
30
Scan duration (minutes)
OC-ME + ME-ICA
OC-ME + ICA-AROMA
TE2 + ICA-AROMA
Cast-Induced Plasticity (N=3)
Midnight Scan Club (N=10)
MyConnectome (N=1)

Figure S3. Related to Figure 3. Reliability of functional connectivity estimates in sub-ME03 and sub-ME04. The purpose of this analysis was to test whether the enhanced FC reliability observed in sub-ME01 and sub-ME02 could be replicated in other individuals. Each participant underwent 3 hours of scanning using a multi-echo fMRI sequence (12 x 14.5 minute scans) over a period of six months. Reliability maps were calculated using the three different denoising strategies, leveraging both (OC-ME + ME-ICA), one (OC-ME + ICA-AROMA), or no (TE_2 + ICA-AROMA) advantages of a multi-echo fMRI sequence. Time x reliability curves (Fig. S3B) show the average reliability value obtained in cortex, subcortical structures (accumbens, amygdala, caudate, hippocampus, pallidum, putamen, and thalamus), and cerebellum given different scan durations. Curves from the three independent single-echo datasets were again provided as comparators). This analysis yielded results consistent with those observed in sub-ME01 and sub-ME02 – the OC-ME and ME-ICA procedures enhanced the reliability of FC. When using the full scan duration, 32% and 72% of cortex exhibited reliable (> 0.7) FC in sub-ME03 and sub-ME04, respectively. One sample t-tests revealed that 10 minutes of OC-ME + ME-ICA data yielded FC estimates that were more reliable than those derived from 3x as much single-echo Midnight Scan Club and Cast-induced Plasticity data in cortex [$t(12) = 3.49$, $p=0.004$, Cohen's $d = 0.97$] and cerebellum [$t(12) = 3.67$, $p=0.003$, Cohen's $d = 1.03$]. In subcortex, 10 minutes of OC-ME + ME-ICA data yielded rsFC estimates more reliable than those derived from an equivalent amount of single-echo data [$t(12) = 6.20$, $p<0.001$, Cohen's $d = 0.81$]. These findings are consistent with those from our analysis of sub-ME01 and sub-ME02 (Fig. 3).

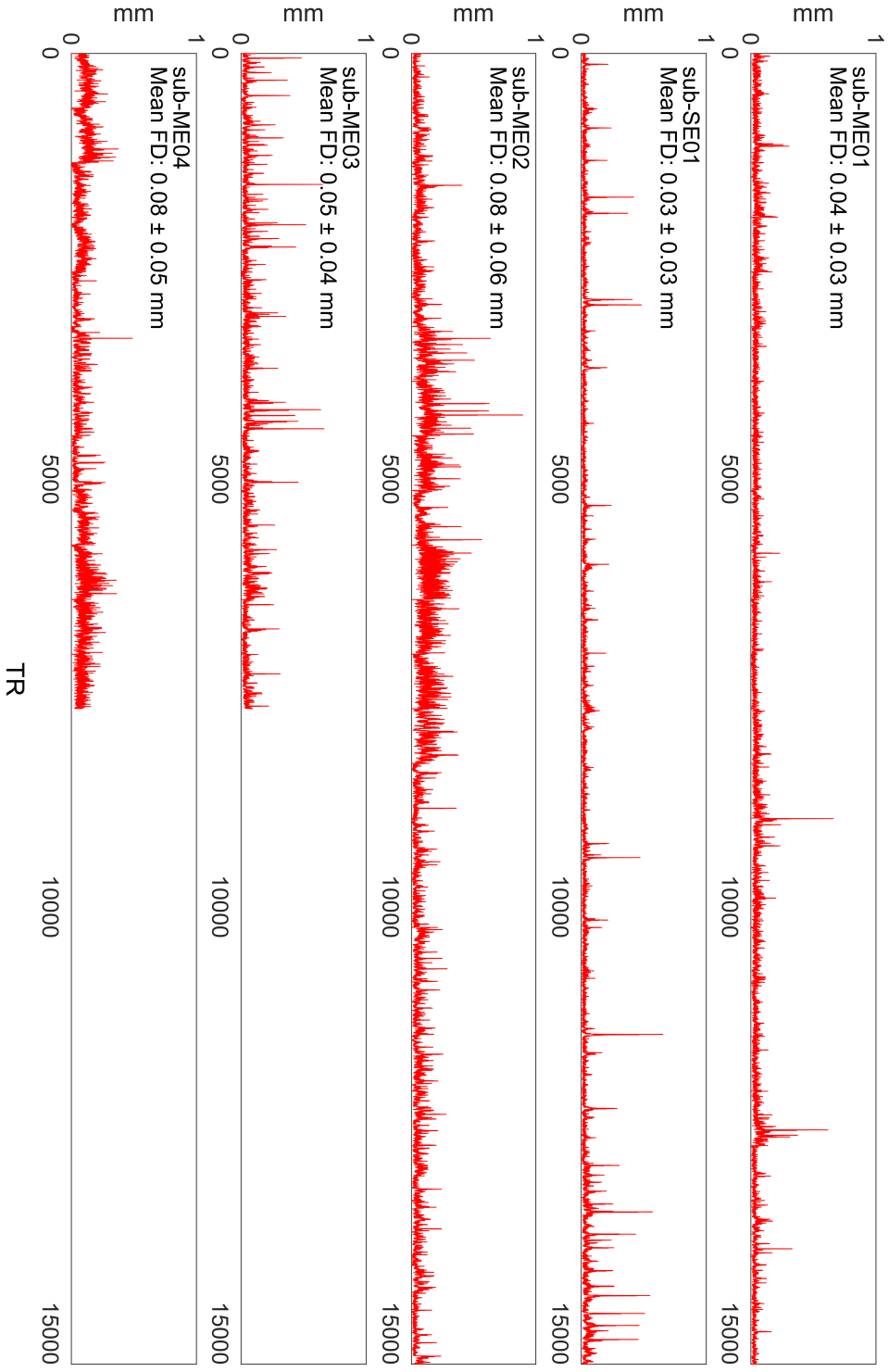
sub-ME01
Mean FD: 0.04 ± 0.03 mm
sub-SE01
Mean FD: 0.03 ± 0.03 mm
sub-ME02
Mean FD: 0.08 ± 0.06 mm
sub-ME03
Mean FD: 0.05 ± 0.04 mm
sub-ME04
Mean FD: 0.08 ± 0.05 mm
mm
0
1
5000
10000
15000
TR

Figure S4. Related to Figure 3. Head movement for all four study participants summarized using concatenated frame-wise displacement (FD) traces. Multiple formulations of FD are shown to convey the effect of the stopband filter ("Filtered FD 1-TR" vs. "Not Filtered FD-1TR") and over 2-TRs ("Filtered FD 2-TRs" versus "Filtered FD 1-TR"). Note that sub-SE01 is participant sub-ME01, but scanned using a separate fast-TR single-echo sequence.

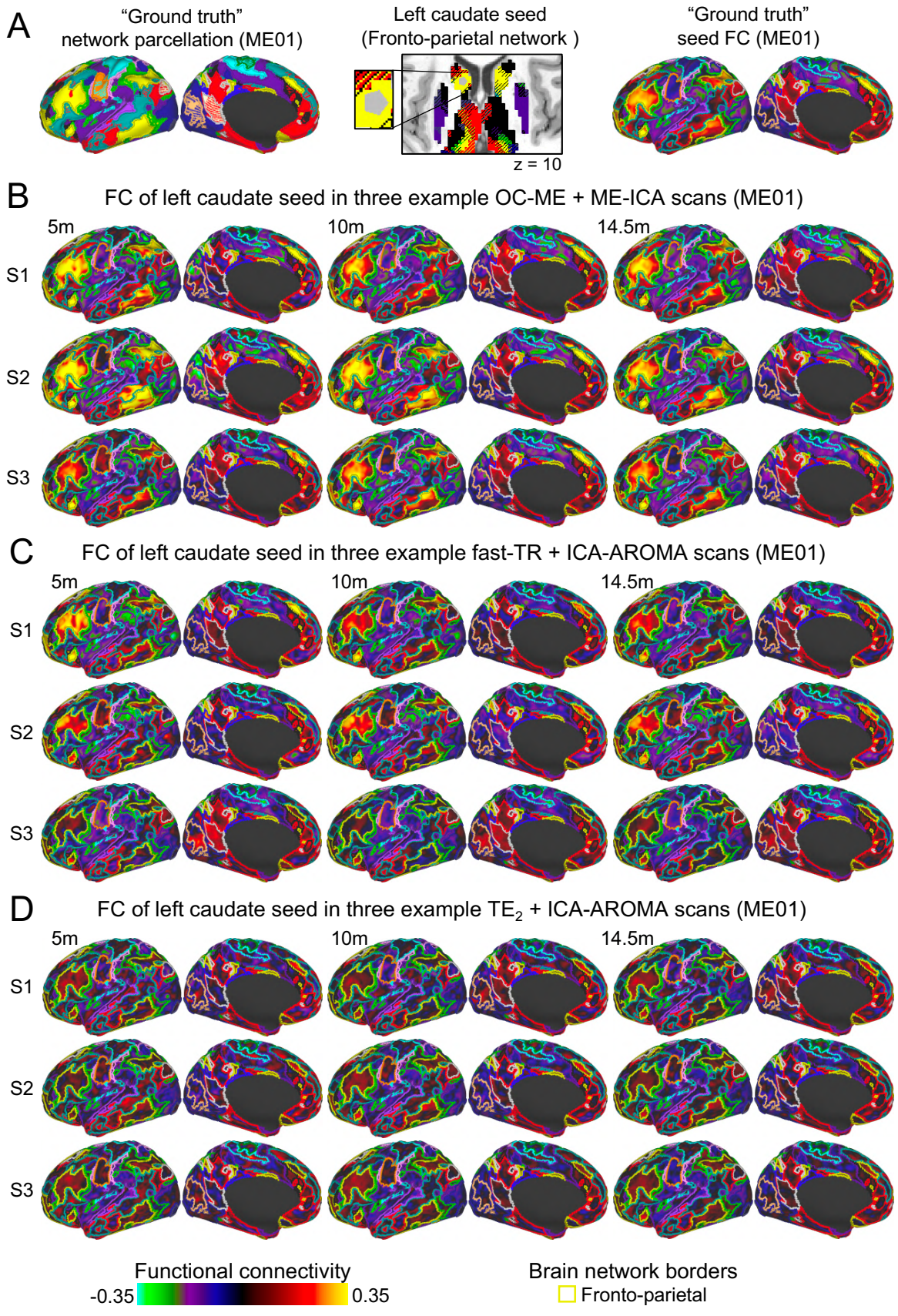
A
"Ground truth" network parcellation (ME01)
Left caudate seed (Fronto-parietal network)
z = 10
"Ground truth" seed FC (ME01)
B
FC of left caudate seed in three example OC-ME + ME-ICA scans (ME01)
5m
10m
14.5m
S1
S2
S3
C
FC of left caudate seed in three example fast-TR + ICA-AROMA scans (ME01)
5m
10m
14.5m
S1
S2
S3
D
FC of left caudate seed in three example TE2 + ICA-AROMA scans (ME01)
5m
10m
14.5m
S1
S2
S3
Functional connectivity
-0.35
0.35
Brain network borders
Fronto-parietal

Figures S5. Related to Figure 4. FC of seed region in left caudate in participant ME01 when using different amounts of multi-echo (OC-ME + ME-ICA) and single-echo data (TE_2 + ICA-AROMA, Fast-TR SE + ICA-AROMA) from 3 example scans. S = scan.

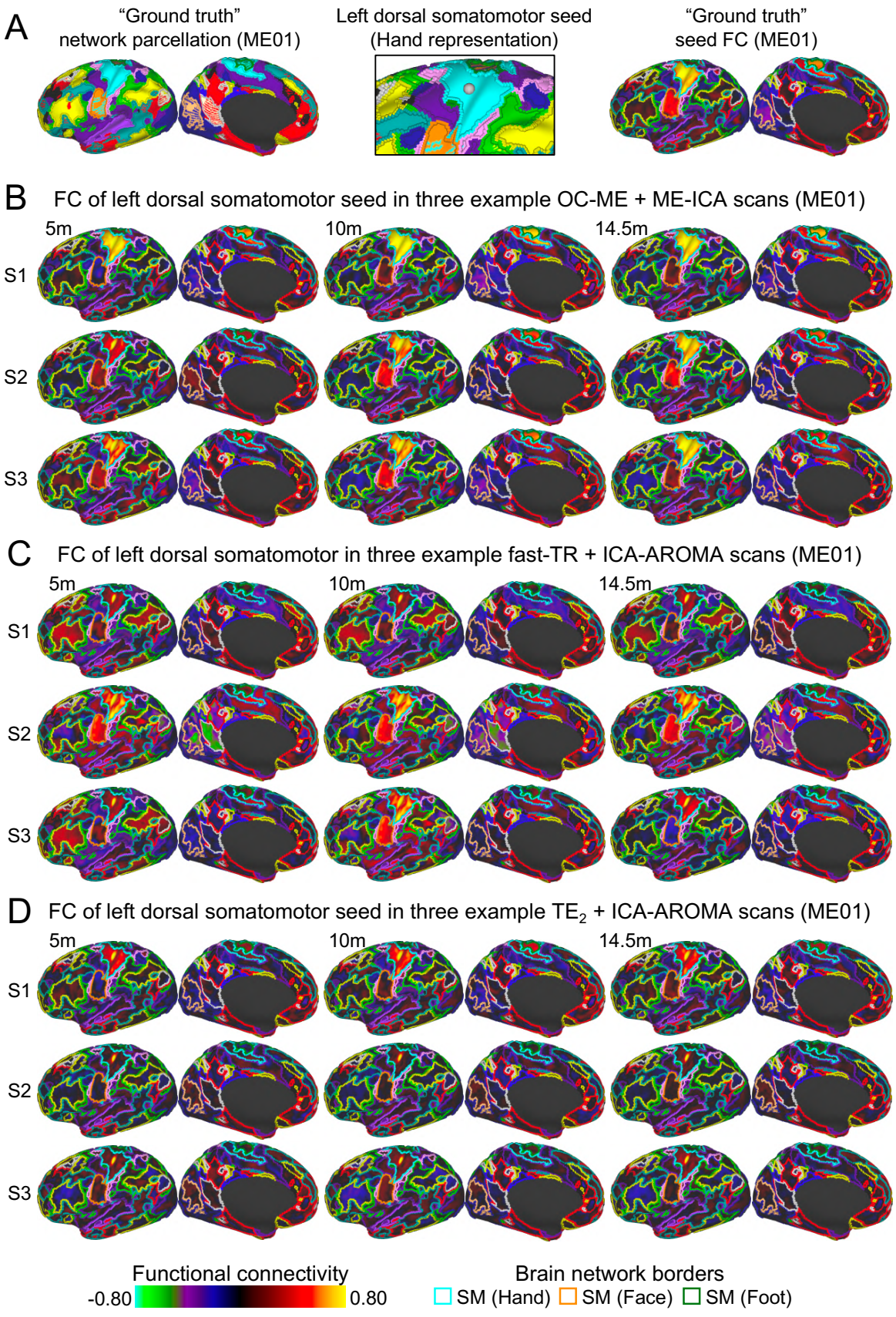
A
"Ground truth" network parcellation (ME01)
Left dorsal somatomotor seed (Hand representation)
"Ground truth" seed FC (ME01)
B
FC of left dorsal somatomotor seed in three example OC-ME + ME-ICA scans (ME01)
5m
10m
14.5m
S1
S2
S3
C
FC of left dorsal somatomotor in three example fast-TR + ICA-AROMA scans (ME01)
5m
10m
14.5m
S1
S2
S3
D
FC of left dorsal somatomotor seed in three example TE2 + ICA-AROMA scans (ME01)
5m
10m
14.5m
S1
S2
S3
Functional connectivity
-0.80
0.80
Brain network borders
SM (Hand)
SM (Face)
SM (Foot)

139

Figures S6. Related to Figure 4. FC of seed region in left dorsal somatomotor cortex in participant ME01 when using different amounts of multi-echo (OC-ME + ME-ICA) and single-echo data (TE_2 + ICA-AROMA, Fast-TR SE + ICA-AROMA) from 3 example scans. S = scan.

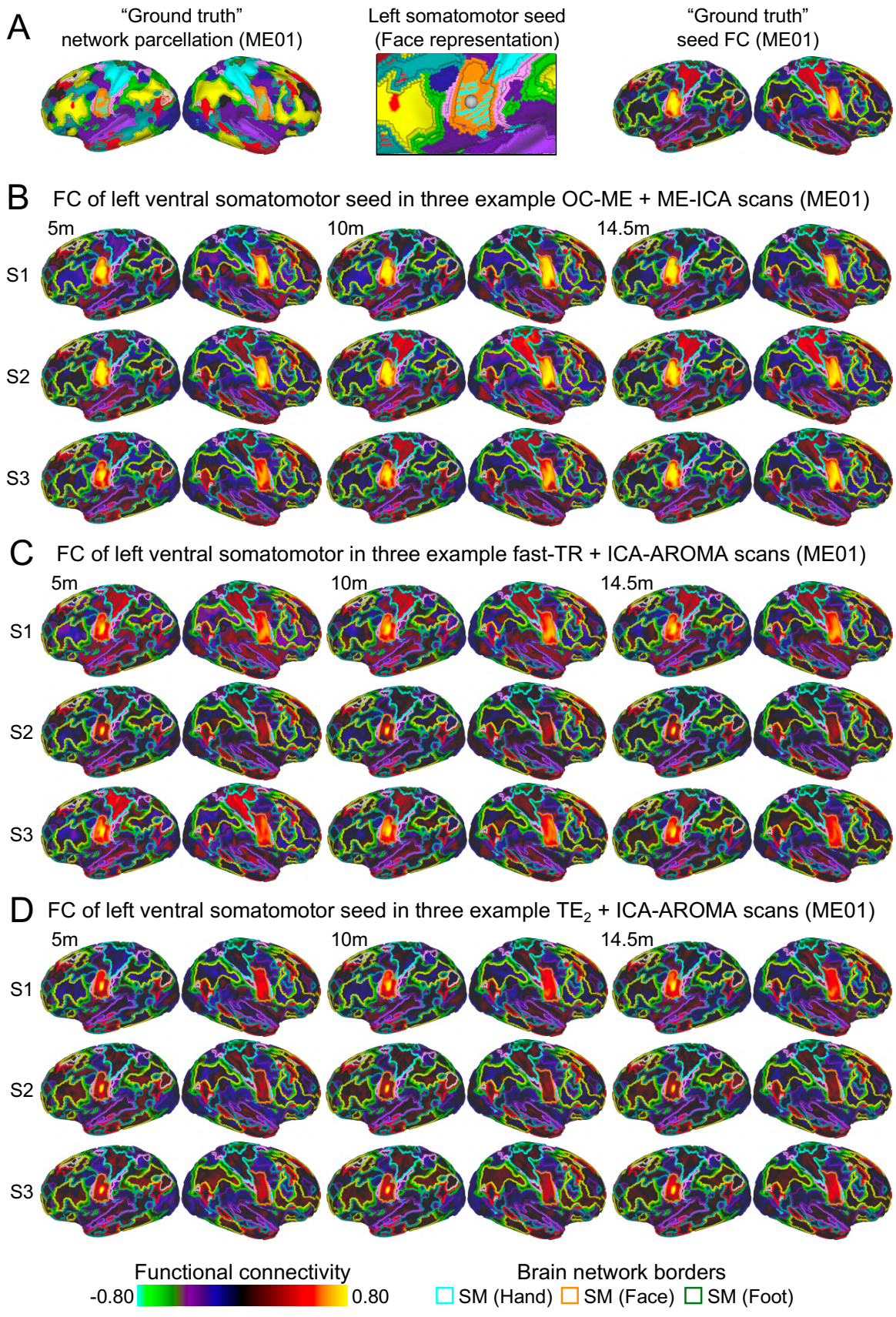
A
"Ground truth" network parcellation (ME01)
Left somatomotor seed (Face representation)
"Ground truth" seed FC (ME01)
B
FC of left ventral somatomotor seed in three example OC-ME + ME-ICA scans (ME01)
5m
10m
14.5m
S1
S2
S3
C
FC of left ventral somatomotor in three example fast-TR + ICA-AROMA scans (ME01)
5m
10m
14.5m
S1
S2
S3
D
FC of left ventral somatomotor seed in three example TE2 + ICA-AROMA scans (ME01)
5m
10m
14.5m
S1
S2
S3
Functional connectivity
-0.80
0.80
Brain network borders
SM (Hand)
SM (Face)
SM (Foot)

144

Figures S7. Related to Figure 4. FC of seed region in ventral somatomotor cortex in participant ME01 when using different amounts of multi-echo (OC-ME + ME-ICA) and single-echo data (TE_2 + ICA-AROMA, Fast-TR SE + ICA-AROMA) from 3 example scans. S = scan.

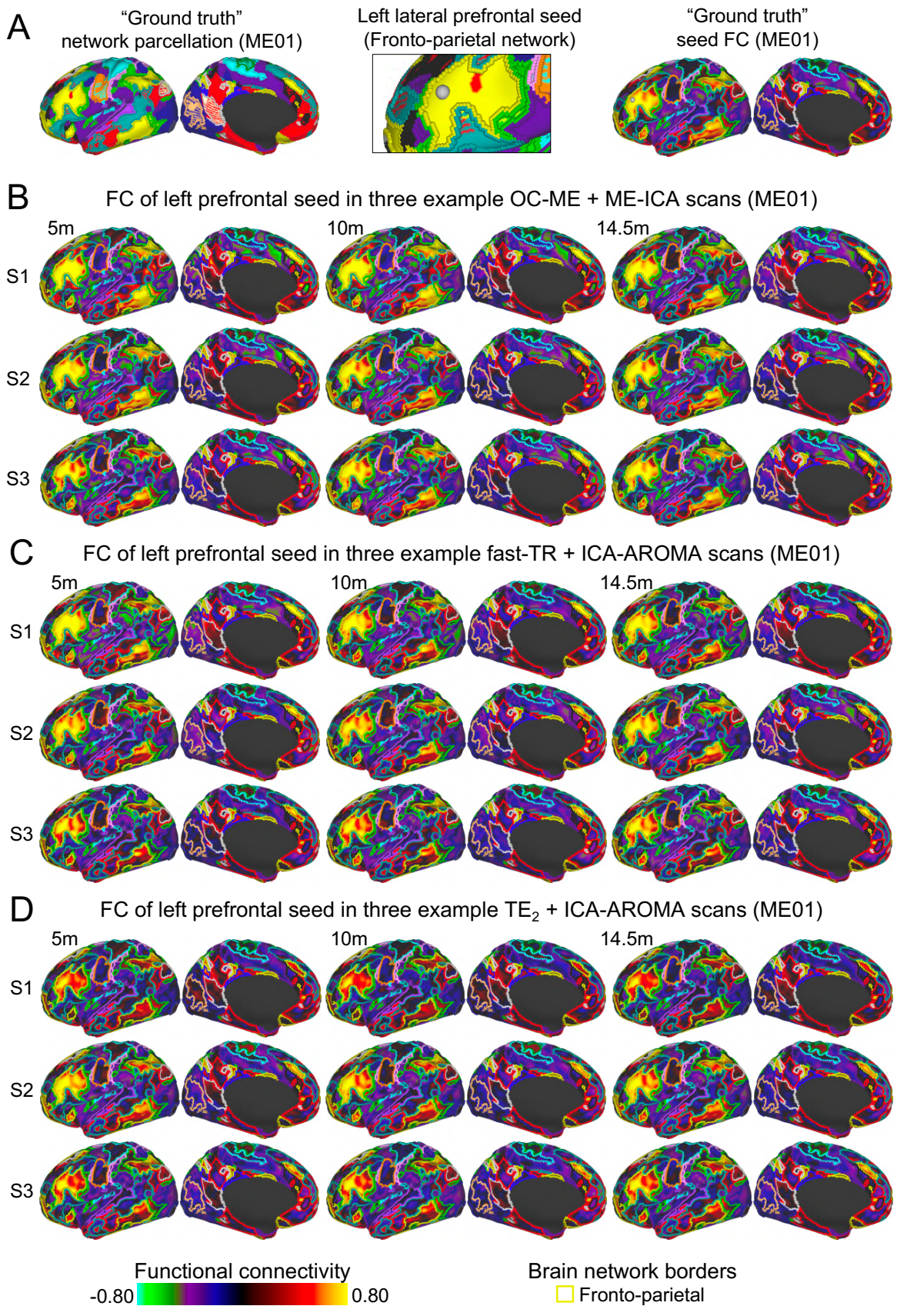
A
"Ground truth" network parcellation (ME01)
Left lateral prefrontal seed (Fronto-parietal network)
"Ground truth" seed FC (ME01)
B
FC of left prefrontal seed in three example OC-ME + ME-ICA scans (ME01)
5m
10m
14.5m
S1
S2
S3
C
FC of left prefrontal seed in three example fast-TR + ICA-AROMA scans (ME01)
5m
10m
14.5m
S1
S2
S3
D
FC of left prefrontal seed in three example TE2 + ICA-AROMA scans (ME01)
5m
10m
14.5m
S1
S2
S3
Functional connectivity
-0.80
0.80
Brain network borders
Fronto-parietal

149

Figures S8. Related to Figure 4. FC of seed region in lateral prefrontal cortex in participant ME01 when using different amounts of multi-echo (OC-ME + ME-ICA) and single-echo data (TE_2 + ICA-AROMA, Fast-TR SE + ICA-AROMA) from 3 example scans. S = scan.

Table 1. Related to Star Methods. Summary of the sequence parameters associated with each of the datasets used in this investigation.

Dataset	Scanner Model	Spatial Resolution	Repetition Time (TR)	Echo Time (TE)	Multi-band Factor	Number of volumes
Midnight Scan Club	Siemens TRIO 3T	4 x 4 x 4 mm	2200 ms	TE_1: 27 ms	None	818
Cast-induced Plasticity	Siemens Prisma 3T	2.6 x 2.6 x 2.6 mm	1100 ms	TE_1: 33 ms	4	1636
MyConnectome	Siemens Skyra 3T	2.4 x 2.4 x 2.4 mm	1160 ms	TE_1: 30 ms	4	518
Multi-Echo	Siemens Magnetom Prisma 3T	2.4 x 2.4 x 2.4 mm	1355 ms	TE_1: 13.40 ms TE_2: 31.11 ms TE_3: 48.82 ms TE_4: 66.53 ms TE_5: 84.24 ms	6	640
“Fast-TR” Singe-Echo	Siemens Magnetom Prisma 3T	2.4 x 2.4 x 2.4 mm	800 ms	TE_1: 30 ms	6	1084